J|A|C|S
ARTICLES
Published on Web 05/26/2005

CdO as the Archetypical Transparent Conducting Oxide. Systematics of Dopant Ionic Radius and Electronic Structure Effects on Charge Transport and Band Structure

Yu Yang,[†,‡] Shu Jin,[†,‡] Julia E. Medvedeva,[‡,§] John R. Ireland,[¶] Andrew W. Metz,[†,‡] Jun Ni,[†,‡] Mark C. Hersam,[¶] Arthur J. Freeman,[*,‡,§] and Tobin J. Marks*[,†,‡]

Contribution from the Department of Chemistry, Materials Research Center, Department of Physics and Astronomy, and Department of Materials Science and Engineering, Northwestern University, Evanston, Illinois 60208-3113

Received February 28, 2005; E-mail: t-marks@northwestern.edu; art@freeman.phys.northwestern.edu

Abstract: A series of yttrium-doped CdO (CYO) thin films have been grown on both amorphous glass and single-crystal MgO(100) substrates at 410 °C by metal−organic chemical vapor deposition (MOCVD), and their phase structure, microstructure, electrical, and optical properties have been investigated. XRD data reveal that all as-deposited CYO thin films are phase-pure and polycrystalline, with features assignable to a cubic CdO-type crystal structure. Epitaxial films grown on single-crystal MgO(100) exhibit biaxial, highly textured microstructures. These as-deposited CYO thin films exhibit excellent optical transparency, with an average transmittance of >80% in the visible range. Y doping widens the optical band gap from 2.86 to 3.27 eV via a Burstein−Moss shift. Room temperature thin film conductivities of 8540 and 17 800 S/cm on glass and MgO(100), respectively, are obtained at an optimum Y doping level of 1.2−1.3%. Finally, electronic band structure calculations are carried out to systematically compare the structural, electronic, and optical properties of the In-, Sc-, and Y-doped CdO systems. Both experimental and theoretical results reveal that dopant ionic radius and electronic structure have a significant influence on the CdO-based TCO crystal and band structure: (1) lattice parameters contract as a function of dopant ionic radii in the order Y (1.09 Å) < In (0.94 Å) < Sc (0.89 Å); (2) the carrier mobilities and doping efficiencies decrease in the order In > Y > Sc; (3) the dopant d state has substantial influence on the position and width of the s-based conduction band, which ultimately determines the intrinsic charge transport characteristics.

Introduction

Transparent conducting oxides (TCOs) have attracted increasing attention over the last two decades as critical components of flat panel displays, solar cells, and low-emissivity windows.[1,2] At present, tin-doped indium oxide (ITO), with a typical electrical conductivity of $3-5 \times 10^3$ S/cm and 85−90% transparency in the visible region, is employed on a huge scale as a transparent electrode in many display technologies. However, there are several drawbacks that cloud its future applicability: (1) the limited availability and high cost of indium; (2) the relatively low conductivity (not suitable for large-area displays); (3) significant optical absorption in the blue−green region (not suitable for many full-color displays); and (4) chemical instability in certain device structures (e.g., corrosion in organic light-emitting diode (OLED) devices). In view of these issues, intense research has been focused on understanding fundamental TCO crystal structure−film microstructure−electronic structure−charge transport−optical transparency relationships and on searching for ITO alternatives that are less expensive and possess comparable or higher conductivity and/or wider optical transparency windows.[1,3]

Recently, CdO-based TCOs have been of interest due to their relatively simple crystal structures, high carrier mobilities, and sometimes nearly metallic conductivities.[1,4−7] Epitaxial growth of Sn-doped CdO thin films on MgO(111) by pulsed laser deposition (PLD) has achieved impressive mobilities and conductivities as high as 607 $cm^2/V\cdot s$ and 42 000 S/cm, respectively, rendering them the most conductive TCO thin films with the highest carrier mobility discovered to date.[6] In addition, Cd_2SnO_4, $CdIn_2O_4$, and CdO−ZnO thin films have been

[†] Department of Chemistry.
[‡] Materials Research Center.
[§] Department of Physics and Astronomy.
[¶] Department of Materials Science and Engineering.

(1) Special Issue on Transparent Conducting Oxides. *MRS Bull.* **2000**, *25* and references therein.
(2) (a) Coutts, T. J.; Mason, T. O.; Perkins, J. D.; Ginley, D. S. *Electrochem. Soc. Proc.* **1999**, 274−288. (b) Wu, X.; Dhere, R. G.; Albin, D. S.; Gessert, T. A.; DeHart, C.; Keane, J. C.; Duda, A.; Coutts, T. J.; Asher, S.; Levi, D. H.; Moutinho, H. R.; Yan, Y.; Moriarty, T.; Johnston, S.; Emery, K.; Sheldon, P. *Proceedings of the NCPV Program Review Meeting*; Lakewood, CO, 2001, Oct. 14−17, pp 47−48. (c) Kawamura, K.; Takahashi, M.; Yagihara, M.; Nakayama, T. European Patent Application, 2003, EP 1271561, A2 20030102, CAN 138:81680, AN 2003:4983.
(3) (a) Wang, R.; King, L. L. H.; Sleight, A. W. *J. Mater. Res.* **1996**, *11*, 1659. (b) Wang, A.; Dai, J.; Cheng, J.; Chudzik, M. P.; Marks, T. J.; Chang, R. P. H.; Kannewurf, C. R. *Appl. Phys. Lett.* **1998**, *73*, 327. (c) Minami, T. *MRS Bull.* **2000**, 38 and references therein. (d) Edwards, D. D.; Mason, T. O.; Sinkler, W.; Marks, L. D.; Goutenoire, F.; Poeppelmeier, K. R. *J. Solid State Chem.* **1998**, *140*, 242−250. (e) Phillips, J. M.; Cava, R. J.; Thomas, G. A.; Carter, S. A.; Kwo, J.; Siegrist, T.; Krajewski, J. J.; Marshall, J. H.; Peck, W. F., Jr.; Rapkine, D. H. *Appl. Phys. Lett.* **1995**, *67*, 2246. (f) Ott, A. W.; Chang, R. P. H. *Mater. Chem. Phys.* **1999**, *58*, 132. (g) Coutts, T. J.; Young, D. L.; Li, X. *J. Vac. Sci. Technol. A* **2000**, *18*, 2646.

10.1021/ja051272a CCC: $30.25

fabricated with impressive conductivities and good optical transparencies for photovoltaic applications.[2] Although the band gap of bulk CdO is only 2.3 eV,[8] leading to relatively poor optical transparency in the short wavelength range, aliovalent metal doping offers the possibility of tuning the electronic structure and the optical band gap through a carrier density dependent Burstein−Moss shift.[5,9] For all these reasons, CdO with a simple cubic rock-salt crystal structure and small conduction electron effective mass represents an ideal model material in which to study the effects of doping on TCO band structure, crystal chemistry, and charge transport.

Various deposition techniques, such as reactive evaporation,[10] solution growth,[11] spray pyrolysis,[12] sputtering,[13] PLD,[6] and MOCVD,[5,7,14] have been employed to grow CdO and CdO-based thin films. For device fabrication, chemical vapor deposition offers many attractive features, such as in situ growth under a variety of atmospheres, low-cost equipment, amenability to large area coverage with high throughput, conformal coverage, easy control of growth chemistry, and the possibility of creating metastable phases.[15] In previous work from this laboratory, undoped and doped CdO thin films were successfully grown by MOCVD using optimized Cd precursors.[5] In-doped CdO thin films grown on glass by MOCVD exhibit conductivities as high as 16 800 S/cm.[5b] In addition, recent studies of Sc-doped CdO thin films reveal that Sc doping significantly contracts the CdO lattice parameter due to its smaller six-coordinate ionic radius, 0.89 versus 1.09 Å for Cd^{2+}.[16] Compared to In-doped CdO films, Sc-doped CdO films exhibit appreciably lower carrier mobilities and concentrations due to the lack of hybridization between the Cd 5s conduction band and Sc 4s states.[5e] Yttrium(III) with a six-coordinate ionic radius of 1.04 Å, which is very close to that of Cd (1.09 Å), has been suggested as an efficient *n*-type dopant in the case of bulk CdO materials.[17,18] It has been reported that for bulk CdO, light Y doping (1−1.5 atom %) increases the carrier density and thus results in lower resistivities in CYO and Cd_2SnO_4 with respect to the undoped analogues. However, CYO thin films have never been prepared and studied.

To further investigate dopant ion size and electronic structure effects on the charge transport properties and electronic band structures of CdO-based TCOs, a series of Y-doped CdO (CYO) thin films have been grown on both amorphous glass and single-crystal MgO(100) substrates by MOCVD, and their electrical and optical properties have been characterized and compared with those of In- and Sc-doped CdO thin films. It will be seen that phase-pure CYO thin films with conductivities of 8540 and 17 800 S/cm on glass and MgO(100), respectively, are obtained at an optimum Y doping level of 1.2−1.3%. To better understand these trends, we report first-principles full potential linear augmented plane wave (FLAPW) electronic band structure calculations within the screened exchange local density approximation (sX-LDA) to systematically compare the structure, electronic, and optical properties of the In-, Sc-, and Y-doped CdO series. Finally, clues for optimizing TCO optical and electrical properties are elucidated from these experimental and theoretical results.

Experimental Section

MOCVD Precursors and Thin Film Growth. CdO-based thin film growth was carried out in the previously described horizontal, cold-wall MOCVD reactor.[19] The volatile metal−organic Cd precursor, Cd(hfa)$_2$(*N*,*N*-DE-*N*′,*N*′-DMEDA) (**1**) (hfa = hexafluoroacetylacetonate, *N*,*N*-DE-*N*′,*N*′-DMEDA = *N*,*N*-diethyl-*N*′,*N*′-dimethylethylenediamine), was prepared from high-purity $Cd(NO_3)_2 \cdot 4H_2O$ (99.999%, Aldrich) as described previously[5d] and was triply vacuum-sublimed. Y(dpm)$_3$ (**2**) (dpm = dipivaloymethanate) was prepared from $Y(NO_3)_3 \cdot 4H_2O$ (99.999%, Aldrich) by a literature procedure.[20] For pure CdO and Y-doped CdO thin film growth, precursor temperature/Ar carrier gas flow rates were optimized by experimentation at: Cd(hfa)$_2$(*N*,*N*-DE-*N*′,*N*′-DMEDA), 85 °C/18 sccm; Y(dpm)$_3$, 90−105 °C/10 sccm. The O_2 oxidizing gas was introduced at 400 sccm by bubbling through distilled water. A system operating pressure of 4.2 ± 0.1 Torr and a substrate temperature of 410 °C established by experimentation were maintained during the thin film deposition. Corning 1737F glass and polished MgO(100) substrates were purchased from Precision Glass and Optics and MTI Corporation, respectively. Both the glass and the MgO(100) substrate surfaces were cleaned with acetone prior to the film deposition and placed side-by-side on the SiC-coated MOCVD susceptor for simultaneous growth experiments.

Film Physical Characterization Measurements. Composition analyses were carried out using inductively coupled plasma atomic emission spectrometry (ICP-AES). Optical transparency measurements were carried out with a Cary 500 UV−vis−NIR spectrophotometer. Film thicknesses were measured with a Tencor P-10 profilometer after etching a step in the film using 5% HCl solution. X-ray diffraction θ-2θ scans of CdO films on glass were obtained with a Rigaku DMAX-A powder diffractometer using Ni-filtered Cu Kα radiation and were calibrated in situ with polycrystalline silicon. Rocking curves and ϕ scans of the epitaxial thin films on MgO(100) substrates were obtained

(4) (a) Kammler, D. R.; Mason, T. O.; Young, D. L.; Coutts, T. J.; Ko, D.; Poeppelmeier, K. R.; Williamson, D. L. *J. Appl. Phys.* **2001**, *90*, 5979−5985. (b) Mason, T. O.; Gonzalez, G. B.; Kammler, D. R.; Mansourian-Hadavi, N.; Ingram, B. J. *Thin Solid Films* **2002**, *411*, 106−114.

(5) (a) Babcock, J. R.; Wang, A.; Metz, A. W.; Edleman, N. L.; Metz, M. V.; Lane, M. A.; Kannewurf, C. R.; Marks, T. J. *Chem. Vap. Deposition* **2001**, *7*, 239. (b) Wang, A.; Babcock, J. R.; Edleman, N. L.; Metz, A. W.; Lane, M. A.; Asahi, R.; Dravid, V. P.; Kannewurf, C. R.; Freeman, A. J.; Marks, T. J. *Proc. Natl. Acad. Sci. U.S.A.* **2001**, *98*, 7113−7116. (c) Asahi, R.; Wang, A.; Babcock, J. R.; Edleman, N. L.; Metz, A. W.; Lane, M. A.; Dravid, V. P.; Kannewurf, C. R.; Freeman, A. J.; Marks, T. J. *Thin Solid Films* **2002**, *411*, 101−105. (d) Metz, A. W.; Ireland, J. R.; Zheng, J. G.; Lobo, R. P. S. M.; Yang, Y.; Ni, J.; Stern, C. L.; Dravid, V. P.; Bontemps, N.; Kannewurf, C. R.; Poeppelmeier, K. R.; Marks, T. J. *J. Am. Chem. Soc.* **2004**, *126*, 8477. (e) Jin, S.; Yang, Y.; Medvedeva, J. E.; Ireland, J. R.; Metz, A. W.; Ni, J.; Kannewurf, C. R.; Freeman, A. R.; Marks, T. J. *J. Am. Chem. Soc.* **2004**, *126*, 13787.

(6) Yan, M.; Lane, M.; Kannewurf, C. R.; Chang, R. P. H. *Appl. Phys. Lett.* **2001**, *78*, 2342−2344.

(7) Zhao, Z.; Morel, D. L.; Ferekides, C. S. *Thin Solid Films* **2002**, *413*, 203−211.

(8) Koffyberg, F. P. *Phys. Rev. B* **1976**, *13*, 4470.

(9) (a) Burstein, E. *Phys. Rev.* **1954**, *93*, 632. (b) Moss, T. S. *Proc. Phys. Soc. A* **1954**, *382*, 775.

(10) (a) Ramakrishna Reddy, K. T.; Sravani, C.; Miles, R. W. *J Cryst. Growth* **1998**, *184*, 1031−1034. (b) Phatak, G.; Lal, R. *Thin Solid Films* **1994**, *245*, 17.

(11) Matsuura, N.; Johnson, D. J.; Amm, D. T. *Thin Solid Films* **1997**, *295*, 260.

(12) (a) Vigil, O.; Vaillant, L.; Cruz, F.; Santana, G.; Morales-Acevedo, A.; Contreras-Puente, G. *Thin Solid Films* **2000**, *361*, 53. (b) Murthy, L. C. S.; Rao, K. S. R. K. *Bull. Mater. Sci.* **1999**, *22*, 953.

(13) (a) Subramanyam, T. K.; Uthanna, S.; Srinivasulu Naidu, B. *Physica Scripta* **1998**, *57*, 317. (b) Lewin, R.; Howson, R. P.; Bishop, C. A.; Ridge, M. I. *Vacuum* **1986**, *36*, 95−98. (c) Gurumurugan, K.; Mangalarj, D.; Narayandass, S. K.; Nakanishi, Y.; Hatanaka, Y. *Appl. Surf. Sci.* **1997**, *114*, 422. (d) Chu, T. L.; Chu, S. S. *J. Electron. Mater.* **1990**, *19*, 1003−1005.

(14) (a) Gulino, A.; Castelli, F.; Dapporto, P.; Rossi, P.; Fragalà, I. *Chem. Mater.* **2002**, *14*, 704−709. (b) Gulino, A.; Dapporto, P.; Rossi, P.; Fragalà, I. *Chem. Mater.* **2002**, *14*, 1441−1444. (c) Gulino, A.; Dapporto, P.; Rossi, P.; Fragalà, I. *Chem. Mater.* **2002**, *14*, 4955.

(15) Schulz, D. L.; Marks, T. J. In *CVD of Non-Metals*; Rees, W. S., Ed.; VCH: New York; pp 39−150.

(16) Shannon, R. D. *Acta Crystallogr.* **1976**, *A32*, 751.

(17) (a) Dou, Y.; Egdell, R. G.; Walker, T.; Law, D. S. L.; Beamson, G. *Surf. Sci.* **1998**, *398*, 241−258. (b) Dou, Y.; Fishlock, T.; Egdell, R. G.; Law, D. S. L.; Beamson, G. *Phys. Rev. B* **1997**, *55*, R13381−R13384.

(18) Gulino A.; Fragalà, I. *J. Mater. Chem.* **1999**, *9*, 2837−2841.

(19) Hinds, B. J.; McNeely, R. J.; Studebaker, D. B.; Marks, T. J.; Hogan, T. P.; Schindler, J. L.; Kannewurf, C. R.; Zhang, X. F.; Miller, D. *J. Mater. Res.* **1997**, *12*, 1214.

(20) Rees, W. S., Jr.; Carris, M. W. *Inorg. Synth.* **1997**, *31*, 302−306.

on a home-built Rigaku four-circle diffractometer with detector-selected Cu Kα radiation. Film surface morphology was examined using a Digital Instruments Nanoscope III atomic force microscope (AFM) operating in the contact mode. Film microstructure was imaged on a Hitachi S4500 FE scanning electron microscope (SEM). Four-probe charge transport data were collected on Bio-Rad HL5500 Hall-effect measurement system at ambient temperature. Variable-temperature Hall effect and four-probe conductivity data were collected between 77 and 340 K using instrumentation described previously.[21]

Theoretical Methods

First-principles electronic band structure calculations on 12.5 atom % In-, Y-, and Sc-doped CdO were performed using the highly precise all-electron full potential linearized augmented plane wave (FLAPW) method[22] that has no shape approximation for the potential and charge density. The exchange−correlation energies were treated via the local density approximation (LDA). Cutoffs of the plane-wave basis (14.4 Ry) and potential representation (81.0 Ry) and expansion in terms of spherical harmonics with $l \leq 8$ inside the muffin-tin spheres were used. The equilibrium relaxed geometries of the crystal structures were determined via total energy and atomic forces minimization for the lattice parameter *a* and the internal atomic positions. Furthermore, to determine accurately the excited-state band structures of In-, Y-, and Sc-doped CdO, we employed the self-consistent screened-exchange local density approximation (sX-LDA),[23] which is known to provide a considerably improved description of the optical properties as compared to the LDA.[22] Cutoff parameters of 10.24 Ry in the wave vectors and $l \leq 3$ inside the muffin-tin spheres were used. Summations over the Brillouin zone were carried out using 10 special *k* points in the irreducible wedge.

Results and Discussion

We first describe Y-doped CdO (CYO) thin film growth by an efficient MOCVD process. Then, CYO film composition, morphology, microstructure, and epitaxy are characterized as a function of doping level using a broad array of complementary physical techniques. In addition, film optical and electrical properties are investigated and compared with those of the In- and Sc-doped CdO analogues grown by the same technique. Finally, first-principles full potential linear augmented plane wave (FLAPW) electronic band structure calculations within the screened exchange local density approximation (sX-LDA) are carried out to compare the structure, electronic, and optical properties of the In-, Sc-, and Y-doped CdO systems.

Film Growth. A series of conductive CYO thin films were grown on 1737F glass and single-crystal MgO(100) at 410 °C and under a 400 sccm O_2 flow rate for 2 h by MOCVD. The growth rates of the film are ∼1.5 nm/min on glass and ∼3.0 nm/min on MgO(100), which are similar to those established for In-[24] and Sc-doped CdO.[5e] The Y doping percentage can be varied from 0 to 4.2% by varying the Y precursor reservoir temperature.

Film Composition, Morphology, Microstructure, and Epitaxy. X-ray diffraction θ-2θ scans were carried out from $2\theta = 25$ to 80°. Figure 1A shows XRD data as a function of Y doping level. As can be seen from the figure, all of the films with Y doping levels up to 4.2% are phase-pure, with a highly

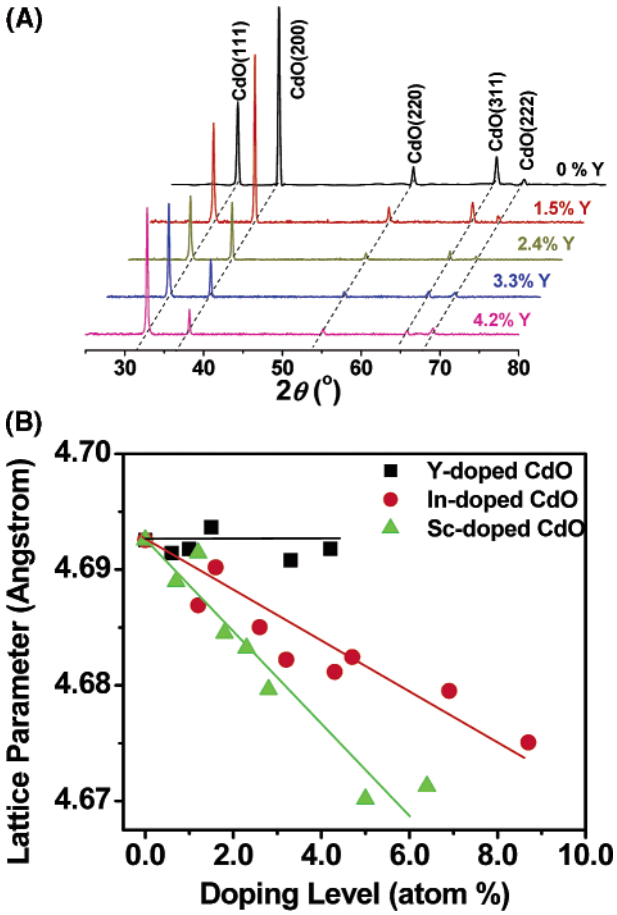

Figure 1. (A) θ-2θ X-ray diffractograms of CYO thin films grown on glass at 410 °C by MOCVD as a function of Y doping level (given in atom %). (B) Lattice parameter changes as a function of dopant size and doping level for Y-, In-, and Sc-doped CdO thin films grown on glass. Lines through the data points are drawn as a guide to the eye.

crystalline fcc CdO structure. No Y_2O_3 or other phases are detected by XRD, indicating Y^{3+} substitutes for the Cd^{2+} in the lattice instead of forming a new phase. This is further evidenced by the fact that the carrier concentration increases progressively with increased Y doping level (see below). It is clear that the presently determined solubility of Y in CdO thin films (∼4.2%) is somewhat greater than that possible in the CdO bulk material (3.5%).[17,18] Furthermore, note that at low doping levels (Y ≤ 2.4%), films on glass grow preferentially with the (*h00*) planes parallel to the surface; while at higher doping levels (Y > 2.4%), (111) reflections dominate. At present, the reason for the change of preferred growth orientation is not immediately evident.

Using polycrystalline silicon as an internal calibration reference, the precise lattice parameters of the MOCVD-derived CYO thin films on glass were determined (Figure 1B). It is found that the lattice parameters are essentially invariant with increasing Y doping level. Note that with the introduction of Y, the lattice dimensions are not expected to change greatly or should shrink slightly, if Y^{3+} ions replace Cd^{2+} in the lattice instead of forming a new phase, since six-coordinate Y^{3+} with an ionic radius of 1.04 Å is slightly smaller than Cd^{2+} (1.09 Å).[16] In addition, the Y^{3+}-induced contraction may be counteracted by an antibonding expansion mechanism (see theoretical discussion below). On the other hand, In^{3+} and Sc^{3+} dopants, having smaller six-coordinate ionic radii of 0.94 and 0.89 Å,

(21) Lyding, J. W.; Marcy, H. O.; Marks, T. J.; Kannewurf, C. R. *IEEE Trans. Instrum. Meas.* **1988**, *37*, 76.
(22) Wimmer, E.; Krakauer, H.; Weinert, M.; Freeman, A. J. *Phys. Rev. B* **1981**, *24*, 864.
(23) Asahi, R.; Mannstadt, W.; Freeman, A. J. *Phys. Rev. B* **1999**, *59*, 7486 and references therein.
(24) In-doped CdO: Jin, S.; Yang, Y.; Medvedeva, J. E.; Ireland, J. R.; Metz, A. W.; Ni, J.; Hersam, M. C.; Freeman, A. R.; Marks, T. J. To be published.

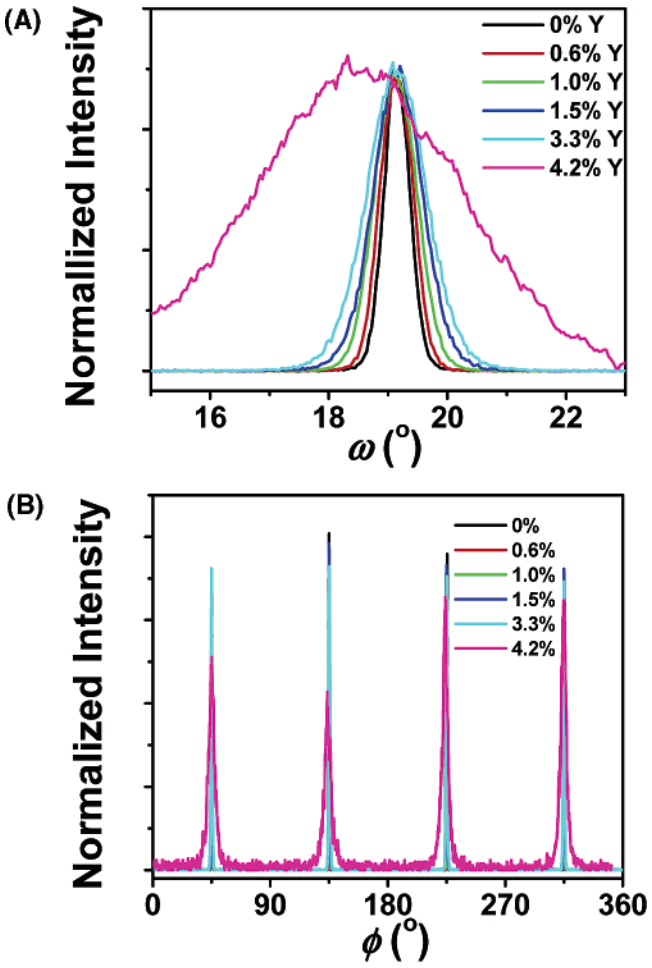

Figure 2. XRD texture analyses of CYO thin films grown on single-crystal MgO(100) as a function of Y doping level: (A) rocking curves measured on the CdO(200) XRD peak; (B) in-plane ϕ scans measured on the CdO-(111) XRD peak with $\chi = 54.7$. Y doping level given in atom %.

respectively, shrink the lattice monotonically with increases in doping level.[5b,e] However, the shrinkages caused by progressive In and Sc doping are not as large as estimated from simple Vegard's law considerations, likely due to compensation by the antibonding character of the conduction band formed from Cd 5s and O 2p states (see theoretical discussion).[5e,24,25]

In contrast to the above results for growth on amorphous glass substrates, all CYO thin films grown on MgO(100) exhibit a highly (200) textured microstructure at all doping levels less than 4.2%. The texture of the thin films is shown in Figure 2. As can be seen from Figure 2A, the rocking curves of the films show good out-of-plane alignment. The full-width at half-maximum (fwhm) increases from 0.5° for pure CdO films to 1.0° at 3.3 atom % Y doping, and to 3.5° at 4.2 atom % Y doping, indicating that the crystallinity decreases with the increase in Y doping. The in-plane orientation was investigated by ϕ scans of the CdO(111) reflection at $\chi = 54.7°$, and data are shown in Figure 2B. The clear 4-fold rotational symmetry of the CdO(111) reflections together with the small fwhm values (0.8° for pure CdO, 1.2° for CYO at 3.3% Y doping) reveals excellent in-plane orientation of the films. The orientation relations between the CYO thin films and the MgO(100) substrates is therefore CdO(100)||MgO(100).

(25) Medvedeva, J. E.; Freeman, A. J. To be published.

SEM surface images in Figure 3 show that the as-deposited CYO thin films grown on glass are densely packed with a heavily grained structure. At low Y doping levels (≤1.5%), films on glass and MgO(100) are all very uniform with rounded grains in plan view. With the Y doping increased to 2.4 and 4.2%, the grains of the films on glass are largely triangular in shape, suggesting that the (111) planes are parallel to the surface, which agrees well with the XRD analysis alluded to above. Furthermore, the SEM images reveal that the grain size decreases with increased Y doping level, similar to the AFM images discussed below. As for the epitaxial films on MgO(100), the films with doping levels ≤1.5% are featureless (single-grained) under SEM and found to be very smooth and uniform under AFM. As the Y doping level is increased to ≥2.4%, a grained structure is clearly visible. Contact-mode AFM images of the CYO thin films are shown in Figure 4. AFM images reveal that all the thin films on glass are uniform and smooth, with root-mean-square (RMS) roughnesses of 5−7 nm over a 5 μm × 5 μm area (Figure 4A,C,E). Similar to the SEM observations, the AFM images show that the grain size of the films decreases with increasing Y doping levels. As for the CYO films grown on MgO(100), the surface roughness of the films is strongly dependent on the doping level. The RMS roughness is found to be 1−2 nm when the doping level is ≤1.5% (Figure 4B,D) and 4−7 nm when the doping level is >1.5% (Figure 4F).

Film Optical and Electrical Properties. All as-grown CdO films are light-yellow to the eye but highly transparent. The color becomes lighter with increased Y doping as the band edge shifts to higher energies. Optical transmission spectra of CYO thin films grown on glass are shown in Figure 5A. For CYO thin films with thicknesses of ~200 nm, the average transmittance at 550 nm is ~85%. With an increase of Y doping level, the band edges are found to be dramatically blue-shifted, doubtless due to the Burstein−Moss effect.[9] Simultaneously, the plasma edges shift to the blue, owing to the increase of free carrier concentration with increased doping level. Band gap estimates were derived from the optical transmission spectra by extrapolating the linear portion of the plot of $(\alpha h\nu)^2$ versus $h\nu$ to $\alpha = 0$ (Figure 5B). It is found that the band gap increases from 2.86 to 3.27 eV with an increase in Y doping from 0 to 4.2%.

As in other aliovalent metal-doped CdO materials investigated to date, all of the Y-doped CdO film samples exhibit *n*-type conductivity as determined by negative Hall coefficients. Figure 6 shows the temperature dependence of thin film charge transport properties for a 1.3 atom % CYO film on MgO(100), which achieves the highest observed conductivity of 17 800 S/cm. Similar to In- and Sc-doped CdO,[5b,e] the mobilities and conductivities of CYO films are independent of temperature in the low-temperature region (<100 K), suggesting that neutral impurity scattering (NIS) and/or ionized impurity scattering (IIS) processes are dominant (see below). In the high-temperature region (>100 K), the mobility and conductivity decrease with increasing temperature, suggesting that lattice vibration scattering (LVS), which is temperature-dependent, has now become an important scattering contributor.

Electrical conductivity, mobility, and carrier concentration data for as-grown CdO thin films as a function of Y, In, and Sc doping levels are compared in Figure 7. For the present Y-doped CdO films, with the increase of Y doping, the carrier concentra-

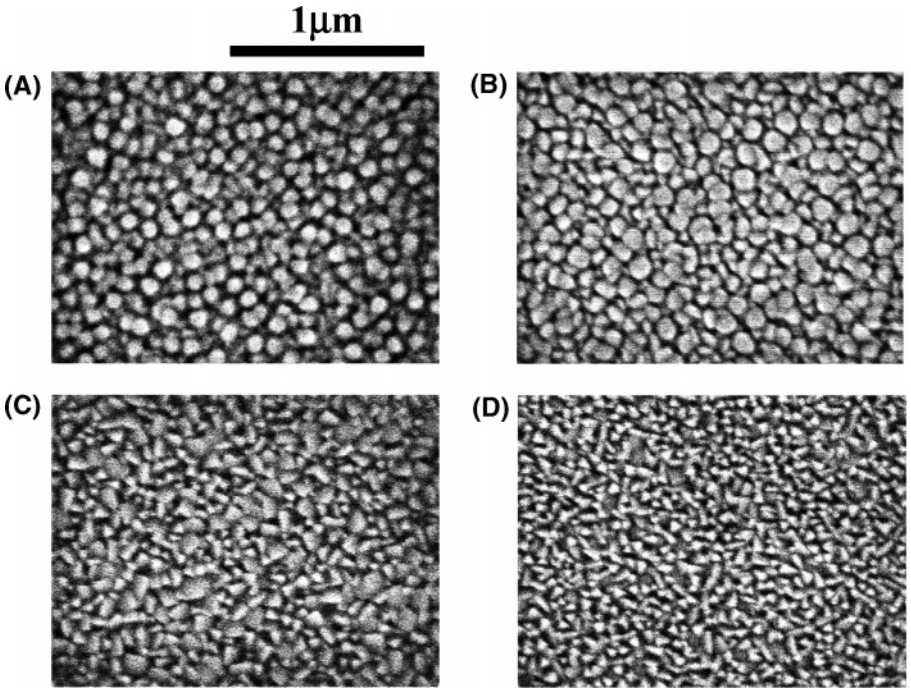

Figure 3. SEM images of CYO thin films on glass as a function of Y doping (given in atom %): (A) 0.6%; (B) 1.5%; (C) 2.4%; (D) 4.2%.

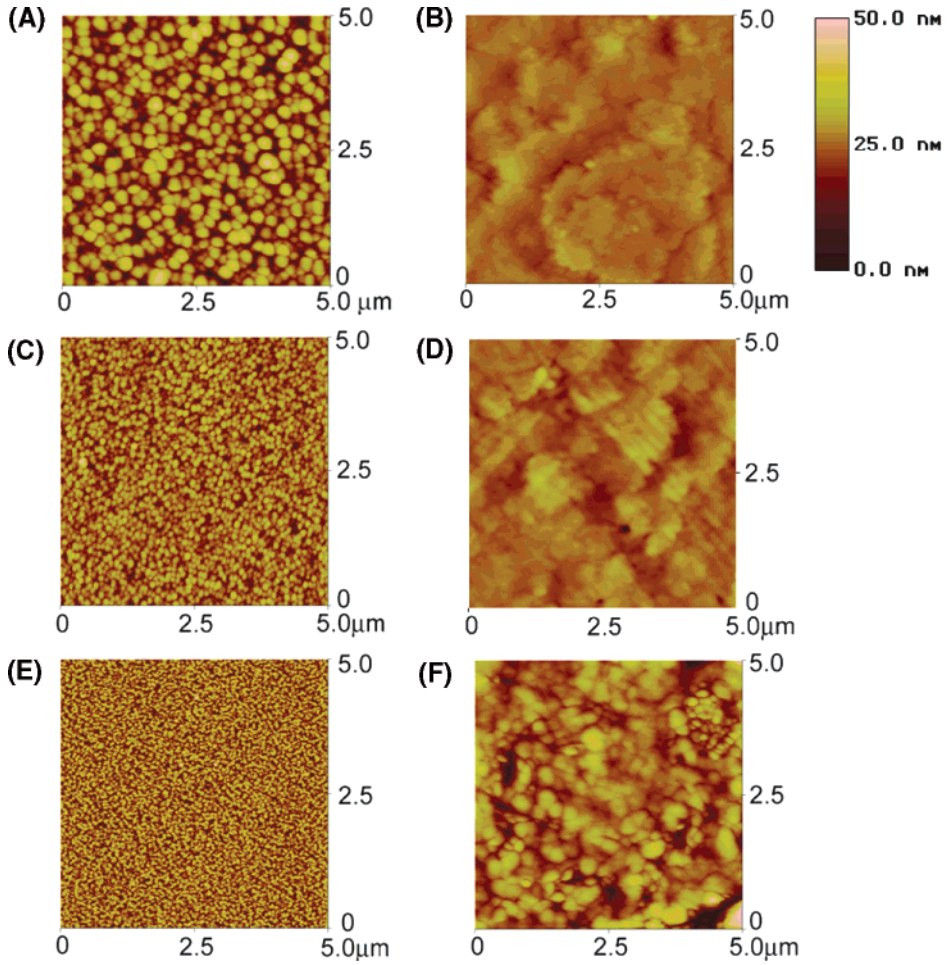

Figure 4. AFM images of CYO thin films as a function of Y doping level (given in atom %): (A) 0.6% Y-doped CdO on glass, RMS roughness = 7.2 nm; (B) 0.6% Y-doped CdO on MgO(100), RMS roughness = 1.9 nm; (C) 1.5% Y-doped CdO on glass, RMS roughness = 5.1 nm; (D) 1.5% Y-doped CdO MgO(100), RMS roughness = 1.1 nm; (E) 2.4% Y-doped CdO on glass, RMS roughness = 6.9 nm; (F) 2.4% Y-doped CdO on MgO(100), RMS roughness = 5.7 nm.

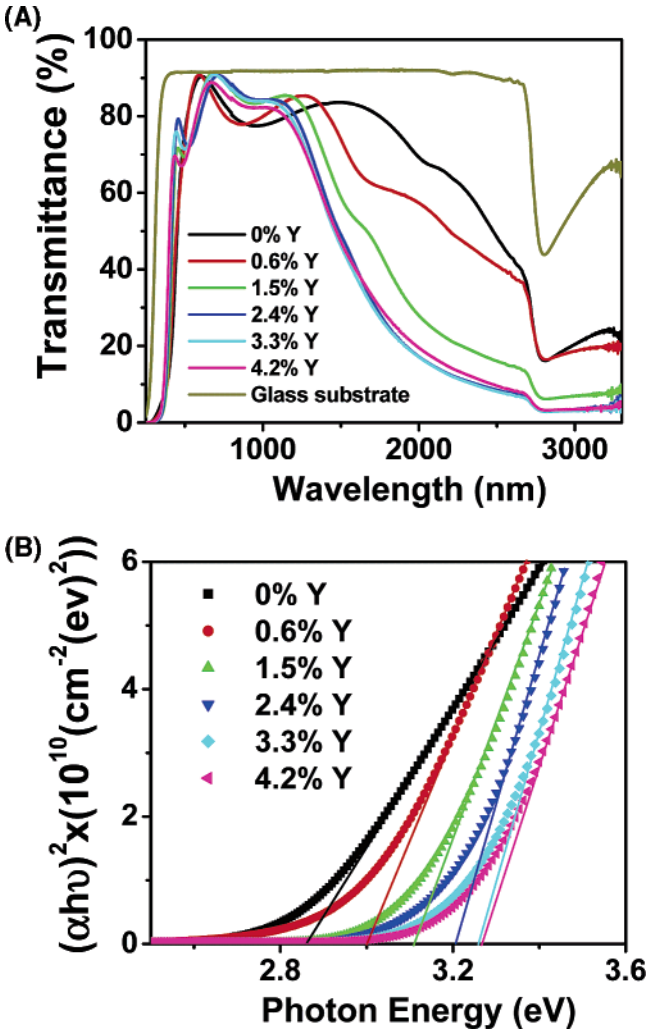

Figure 5. Optical characterization of MOCVD-derived CYO thin films grown on glass as a function of Y doping: (A) optical transmission spectra; (B) band gap estimations.

tion increases from 2.3×10^{20} cm^{-3} for pure CdO thin films on glass to 7.0×10^{20} cm^{-3} at ~2.4% Y doping. The mobility, however, drops precipitously with increased Y doping. It is clear from these data that Y^{3+} ions behave as effective dopants by replacing Cd^{2+} sites in the lattice and donating electrons to act as charge carriers. However, at doping levels greater than 2.4%, the carrier density plateaus and the mobilities decline substantially, indicating that some of the Y dopant sites may not readily be ionized and/or do not contribute to the mobile charge carriers. In addition, excess Y doping appears to degrade the thin film crystallinity and increase carrier scattering, thereby decreasing carrier mobility and conductivity. Compared with In and Sc doping, much less Y can be effectively doped into the CdO lattice. Thin films with maximum conductivities of 8540 and 17 800 S/cm on glass and MgO(100), respectively, are obtained at 1.2−1.3% Y doping. Compared with films on glass, CYO films on MgO(100), at the same doping level, exhibit similar doping level-dependent trends but exhibit much greater carrier concentrations and mobilities (Figure 7), indicating that the epitaxial films possess fewer scattering centers and higher doping efficiency due to their highly textured microstructure/enhanced crystalline perfection, similar to behavior found for epitaxial CdO on MgO(100)[5d] and epitaxial ITO on single-crystal YSZ.[26] In addition, the comparison of charge transport properties for In-, Y-, and Sc-doped CdO given in Figure 7 shows that the carrier mobilities and doping efficiencies decrease in the order In > Y > Sc.

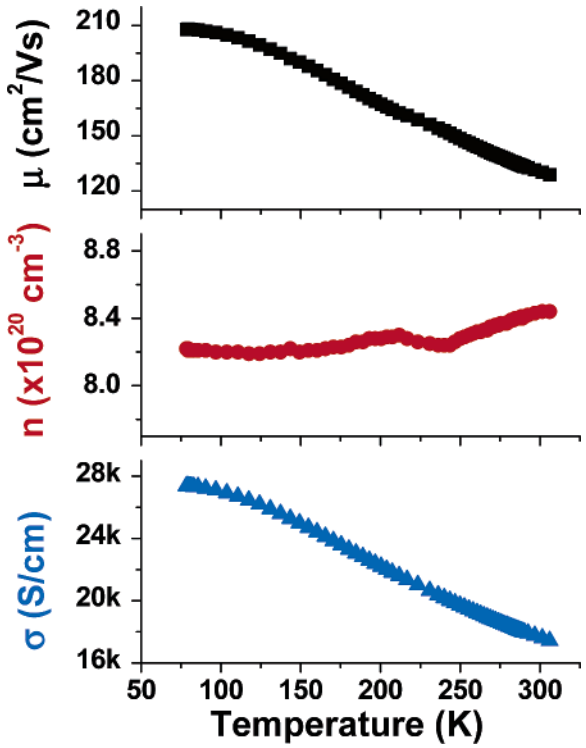

Figure 6. Variable-temperature electrical conductivity and Hall-effect measurements for 1.3 atom % Y-doped CdO thin film on MgO(100): carrier mobility (■, top), carrier concentration (●, middle), and electrical conductivity (▲, bottom).

Band Structure Calculations. The total energy FLAPW method was used to carry out full optimization of the CYO crystal structure (both the lattice and internal parameters were optimized) at 12.5 atom % Y doping. We find that the CYO lattice parameter, $a = 4.67$ Å, is slightly larger than that of pure CdO (4.66 Å, as obtained from a separate calculation), despite the fact that the six-coordinate ionic radius of Y^{3+} (1.04 Å) is somewhat smaller than that of Cd^{2+} (1.09 Å). This finding can be explained by comparison of the calculated structural and electronic properties of In-, Y-, and Sc-doped CdO. In Table 1, we present the LDA-optimized lattice parameters and relaxed distances between the Cd or X (X = In, Y, or Sc) atom and its nearest O neighbors, D_{Cd-O} and D_{X-O}, for In-, Y-, and Sc-doped CdO. It can be seen that the calculated change in the lattice parameter for different dopants correlates well with their ionic radii, namely, Y^{3+} (1.04 Å) > In^{3+} (0.94 Å) > Sc^{3+} (0.89 Å). Furthermore, it is found that smaller dopant ionic radii result in weaker Cd 5s−O 2p hybridization due to relaxation of the oxide anions around the dopant cations. Therefore, any shrinkage in the lattice parameter due to the larger Y^{3+} ion is well compensated by the aforementioned antibonding expansion mechanism, in contrast to Sc-doped CdO, where the lattice is significantly compressed due to the very much smaller ionic radius of Sc^{3+}, hence again inducing diminished s−p hybridization between the Cd 5s and O 2p orbitals. These results are in good agreement with the experimental findings reported above

(26) Taga, N.; Odaka, H.; Shigesato, Y.; Yasui, I.; Kamei, M.; Haynes, T. E. *J. Appl. Phys.* **1996**, *80*, 978−984.

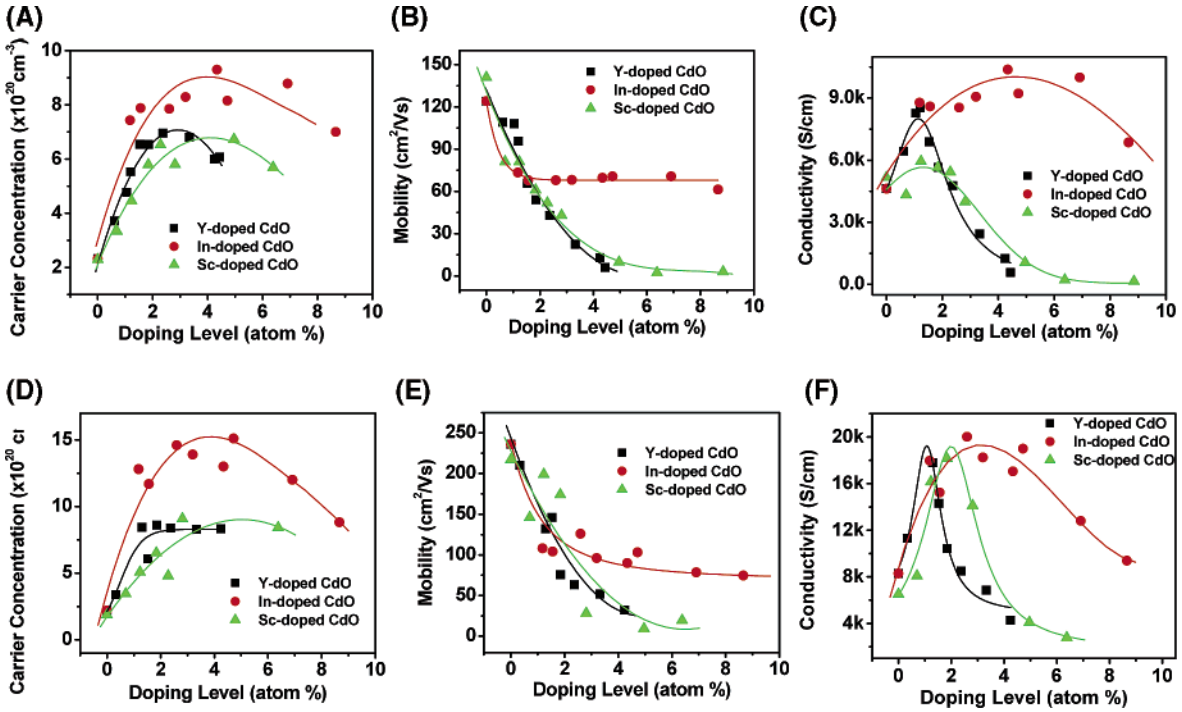

Figure 7. Room temperature four-probe charge transport measurements for Y-, In-, and Sc-doped CdO thin films on glass: (A) carrier concentration, (B) mobility, (C) conductivity; and on MgO(100): (D) carrier concentration, (E) mobility, (F) electrical conductivity. Lines are a guide to the eyes.

Table 1. Calculated Optimized Lattice Parameters (*a*); Relaxed Distances between the Cd (X = In, Y, or Sc) Atom and Its Nearest O Neighbors (D_{Cd-O}, D_{X-O}); Optical Band Gap Values (E_g) in the (Δ) [100], (Λ) [110], and (Σ) [111] Directions; Width of the Single Dispersed Band (*E*); Electron Velocities (*V*) at the Fermi Level in the (Δ) [100], (Λ) [110], and (Σ) [111] Directions; and Density of States at the Fermi Level ($N(E_F)$) for In-, Y-, and Sc-Doped CdO

dopant	In	Y	Sc
a, Å	4.66	4.67	4.63
D_{X-O}, Å	2.24	2.28	2.18
D_{Cd-O}, Å	2.42	2.39	2.45
E_g (Δ), eV	3.03	3.38	3.02
E_g (Λ), eV	3.68	4.04	3.65
E_g (Σ), eV	3.83	4.17	3.76
Δ*E*, eV	3.91	3.36	2.57
v(Δ), $\times 10^5$ m/s	0.42	0.36	0.19
v(Λ), $\times 10^5$ m/s	0.23	0.21	0.17
v(Σ), $\times 10^5$ m/s	0.12	0.12	0.10
$N(E_F)$	1.16	1.34	2.00

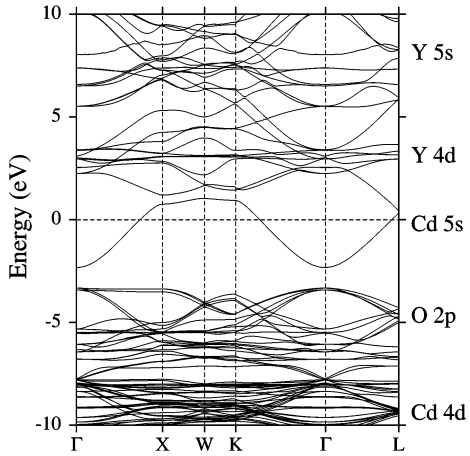

Figure 8. Band structure of 12.5 atom % Y-doped CdO calculated within the sX-LDA formalism along the high-symmetry directions in the Brillouin zone. The origin of the energy is taken at the Fermi level.

and with previous structural results for the In- and Y-doped CdO bulk materials.[17,27]

The band structure of CYO at 12.5 atom % Y doping calculated within the sX-LDA formalism is shown in Figure 8. Despite a rather small (indirect) band gap of ~1 eV in pure CdO,[5c] Y doping results in a Burstein−Moss shift which significantly widens the optical transparency window so that the energies of the intense interband transitions from the valence band are above the visible range in energy; the calculated sX-LDA band gap energies, E_g (cf. Table 1), which determine the optical transparency of CYO, are found to be 3.38, 4.04, and 4.17 eV in the [100], [110], and [111] directions, respectively. The minimum band gap value is in good agreement with the present experimental result (3.27 eV). As expected, LDA alone is found to underestimate the band gap energies, yielding 2.51, 3.13, and 3.17 eV in the [100], [110], and [111] directions, respectively. We next compare the sX-LDA results for CYO with those for In- and Sc-doped CdO obtained at the same doping level of 12.5 atom %. In both cases, smaller band gap energies are found, namely, 3.03, 3.68, and 3.83 eV for In doping and 3.02, 3.65, and 3.76 eV for Sc doping in [100], [110], and [111] directions, respectively. This result correlates well with the larger calculated distances between the Cd atom and its neighboring O atoms in In- (2.42 Å) and Sc (2.45 Å)-doped CdO as compared to those in CYO (2.39 Å). Thus, we conclude that a larger ionic radius dopant ion results in a larger optical band gap. More detailed investigations of the optical properties of the In-, Y-, and Sc-doped CdO, including the calculations of the transition matrix elements, will be published elsewhere.[25]

Similar to the cases of In- and Sc-doped CdO,[5b,c,e] the highly dispersed CYO single conduction band, derived mainly from the 5s states of Cd, crosses the Fermi level in the [100] (Δ),

(27) Morozova, L. V.; Komarov, A. V. *Russ. J. Appl. Chem.* **1995**, *68*, 1240.

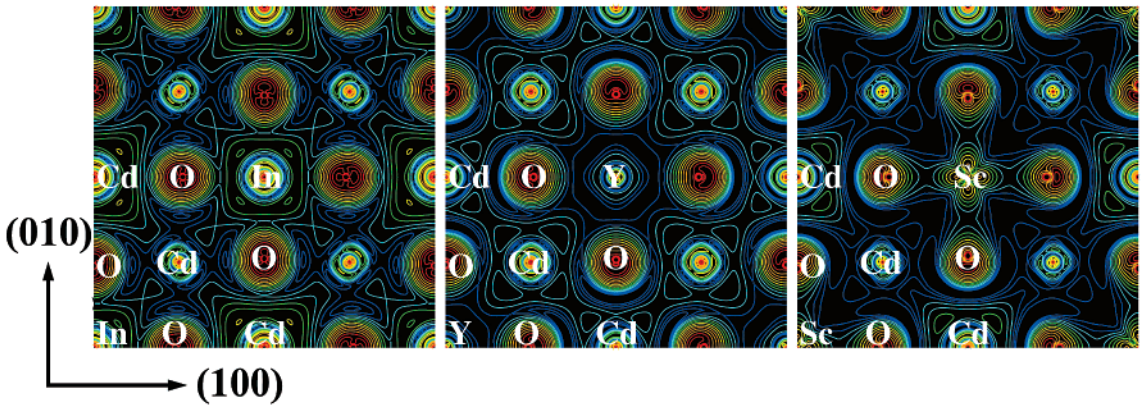

Figure 9. Calculated charge density distribution in the *ab* plane within the energy window of 0.027 eV below the Fermi level for the In-, Y-, and Sc-doped CdO. Atoms within one unit cell are labeled.

[110] (Λ), and [111] (Σ) directions (cf. Figure 8). However, in marked contrast to the case of In doping, the Y 5s and Sc 4s states are found to lie high in the conduction band (at ~8.0 and ~9.5 eV, respectively) and thus do not hybridize with the Cd 5s states. Therefore, the uniform electronic charge density distribution associated with the energy-compatible s-orbital of the In ion is not possible in the Y and Sc cases where the d-orbitals of the dopant ions hybridize only with the p-orbitals of the nearest oxygen neighbors (cf. Figure 9). Consequently, we find that the relative contributions from the oxygen neighbors of the dopant ions to the conduction band, calculated within the energy window from 0.027 eV below the Fermi level, decrease significantly in the order In > Y > Sc (namely, 24, 22, and 12% for the In-, Y-, and Sc-doped CdO, respectively), resulting in charge redistribution and its localization on the Cd ions which contribute 38, 39, and 48% for the In-, Y-, and Sc-doped CdO, respectively. A comparison of the dispersion of the free-electron-like band for In-, Y-, and Sc-doped CdO, given in Figure 10, shows that the width of the band, ΔE (Table 1), significantly narrows in the order In > Y > Sc. This can be explained by the fact that the width of the dispersed band is strongly affected by the presence of the Y 4d or Sc 3d states near the bottom of the conduction band which lies at 3.4 and at 2.0 eV for Y- and Sc-doped CdO, respectively, in contrast to the In case, where the 4d states are fully occupied and lie at −15 eV. Importantly, this dependence of the band dispersion on the dopant identity suggests a decrease in the conductivity, σ, for the above sequence. The conductivity can be expressed as in eq 1:

$$\sigma(\epsilon) = e^2 \sum_k N(\epsilon) v_k^2(\epsilon) \tau(\epsilon) \qquad (1)$$

where e is the electron charge, k the wave vector, ϵ the band energy, $N(\epsilon)$ the density of states, $v_k(\epsilon)$ the group velocity, and $\tau(\epsilon)$ the relaxation time. Assuming $\tau(\epsilon)$ is similar for Y-, In-, and Sc-doped CdO, we can calculate the electron velocities, v, at the Fermi level in the (Δ) [100], (Λ) [110], and (Σ) [111] directions (Table 1). It is found that despite the increase in the density of states at the Fermi level, $N(E_F)$ (Table 1), associated with the lower dispersion of the single band, the electron velocities decrease significantly in the order In > Y > Sc, leading to a pronounced decrease of the conductivity for this sequence. These findings are in excellent agreement with experimental observations on the carrier mobility and conductivity reported above and in previous studies.[5e] Finally, note that for all dopants considered, the largest velocity is in the [100] (Δ) direction, while considerably smaller values are obtained for the [110] (Λ) and [111] (Σ) directions.

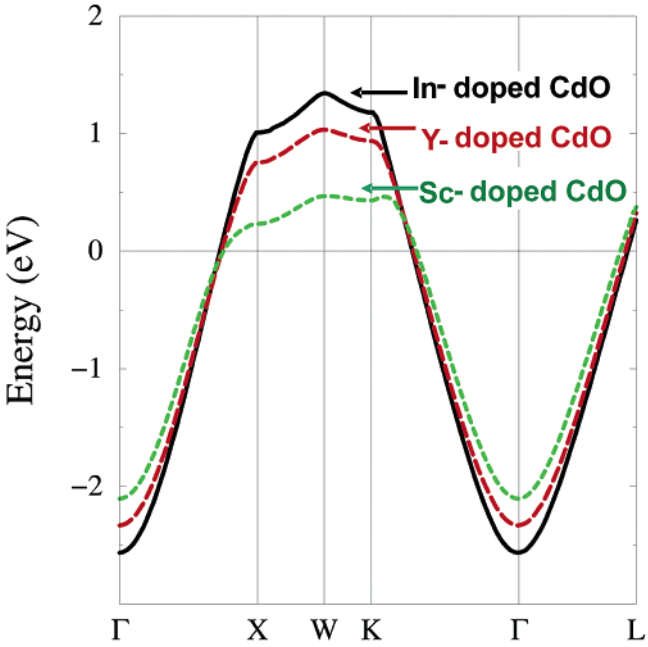

Figure 10. Comparison of the single band dispersion of 12.5 atom % In-doped CdO (solid line), Y-doped CdO (dashed line), and Sc-doped CdO (dotted line) calculated within the sX-LDA formalism. The origin of the energy is taken at the Fermi level.

Conclusions

Highly conductive and transparent CYO thin films have been grown on glass and single-crystal MgO(100) substrates at 410 °C by low pressure MOCVD. The as-deposited CYO thin films exhibit good optical transparency, with an average transmittance of 85% in the visible region. As in the cases of In and Sc doping, Y doping significantly increases the electrical conductivity and widens the optical band gap. Thin films with maximum conductivities of 8540 and 17 800 S/cm on glass and MgO-(100), respectively, are obtained at a Y doping level of 1.2−1.3%. Y doping widens the band gap from 2.86 to 3.27 eV via a Burstein−Moss (B−M) shift. Epitaxial films grown on MgO-(100) also exhibit a biaxial, highly textured microstructure, leading to higher doping efficiency and fewer scattering centers,

which is suggested to be responsible for the higher conductivity versus the films on glass. Both experimental and theoretical results reveal that dopant ion size and electronic configuration have significant influence on the CdO-based TCO crystal and band structures, as well as on the optical and electrical properties. First, In^{3+} (0.94 Å) and Sc^{3+} (0.89 Å), with smaller ion sizes than that of Cd^{2+}(1.09 Å), shrink the lattice parameters; while Y^{3+} (1.04 Å), with similar ion size to that of Cd^{2+}, does not significantly alter the lattice parameter. Second, in marked contrast to In-doped CdO, in the cases of Y and Sc doping, the Cd 5s states do not hybridize significantly with Y 5s and Sc 4s states, respectively. Third, the presence of the "d states" of Y and Sc significantly affects the dispersion of the single band which crosses the Fermi level, resulting in lower mobility as compared to In-doped CdO, which agrees well with experimental observation.

On the basis of the results of the present studies, it can be seen that CdO-based TCO films generally exhibit higher carrier mobility than those of In_2O_3-, ZnO-, and SnO_2-based TCO materials, which can be ascribed to CdO's simple cubic crystal structure, and broadly dispersed, free electron-like Cd 5s-based conduction band. In the doping studies, it is found that the smaller the dopant size, the higher the dopant solubility in the CdO matrix. However, the doping efficiency is strongly dependent on the degree of orbital hybridization between the dopant orbital and Cd 5s states. On the basis of the computational results,[25] we find that dopant ions whose s-orbital states are empty and close to the Cd 5s state in energy, such as Sn^{4+} and Sb^{5+}, should be more effective than those with empty d-orbitals, such as Zr^{4+} and Nb^{5+}. These implications should be applicable to other doped TCO materials, as well, and are currently under investigation. In conclusion, we find that dopant ion size and electronic configuration have substantial influence on the CdO crystal and band structure, especially on the energetic position and width of the highly dispersed conduction band, which provide necessary conditions for creating transparent conducting behavior with doping.

Acknowledgment. This work was supported by the United States Display Consortium (USDC) and by the NSF (CHE-0201767). We acknowledge access to the facilities of the Northwestern Materials Research Center supported by the NSF-MRSEC program (DMR-00760097). Dr. J. Carsello is acknowledged for his assistance with X-ray diffraction measurements.

JA051272A